

Fig. 2. Shapes of coordination polyhedra for (a) Cu(1), and (b) Cu(2). For atomic labelling see Table 1. For symmetry code see Table 2.

The Cu(2) atom of the CuCl_2 molecule is coordinated to four carboxylic O atoms of two neighbouring molecules of the ligand. The coordination distances are comparable to those of Cu(1) (two short, two elongated) (Table 2). Taking into account the two Cl atoms, the coordination sphere for Cu(2) is a completely irregular octahedron where Cl-Cl forms an edge (Fig. 2b). The volumes of both polyhedra despite differing geometry and coordinating elements are very close [$V = 13.68$ (4) and 13.38 (3) \AA^3 for Cu(1) and Cu(2) respectively].

The common O(22) and O(26) atoms of the two coordination spheres cause the molecules of the complex to be joined forming chains parallel to $[101]$. The Cu(1)···Cu(2) and Cu(2)···Cu(1') distances are 4.604 (2) and 4.651 (2) \AA respectively; their angles at

Cu(1) and Cu(2) are 177.28 (3) and 170.78 (3) $^\circ$ respectively.

The authors thank Dr R. A. Koliński for supplying pure samples of the crystals and for valuable discussion. The investigations were supported by grants from the Polish Academy of Sciences, Nos. MR-I.9 and C-1.1.

References

- GLUZIŃSKI, P., KRAJEWSKI, J. W., URBAŃCZYK-LIPKOWSKA, Z., BLEIDELIS, J. & MISHNYOV, A. (1982). *Cryst. Struct. Commun.* **11**, 1589–1592.
- HERCEG, M. & WEISS, R. (1972). *Bull. Soc. Chim. Fr.* pp. 549–551.
- HERCEG, M. & WEISS, R. (1973a). *Acta Cryst.* **B29**, 542–547.
- HERCEG, M. & WEISS, R. (1973b). *Rev. Chim. Minér.* **10**, 509–518.
- International Tables for X-ray Crystallography* (1974). Vol. IV. Birmingham: Kynoch Press.
- KOLIŃSKI, R. A. & MROZIŃSKI, J. (1983). *Polyhedron*, **2**, 1217–1220.
- KRAJEWSKI, J. W., GLUZIŃSKI, P., URBAŃCZYK-LIPKOWSKA, Z. & DOBLER, M. (1983). In preparation.
- METZ, B. & WEISS, R. (1973). *Acta Cryst.* **B29**, 1088–1093.
- MORAS, D., METZ, B., HERCEG, M. & WEISS, R. (1972). *Bull. Soc. Chim. Fr.* pp. 551–555.
- SHELDRIK, G. M. (1976). *SHELX76*. Program for crystal structure determination. Univ. of Cambridge, England.
- UECHI, T., UEDA, I., TAZAKI, M., TAKAGI, M. & UENO, K. (1982). *Acta Cryst.* **B38**, 433–436.
- URBAŃCZYK-LIPKOWSKA, Z., KRAJEWSKI, J. W., GLUZIŃSKI, P., ANDRETTI, G. D. & BOCELLI, G. (1981). *Acta Cryst.* **B37**, 470–473.

Acta Cryst. (1984). **C40**, 781–786

The Structures of the Lanthanide Ethyl Sulfate Enneahydrates, $M(\text{C}_2\text{H}_5\text{SO}_4)_3 \cdot 9\text{H}_2\text{O}$ [$M = \text{La} - \text{Lu}$ (except Pm)], at 171 K

BY ROGER E. GERKIN AND WILLIAM J. REPPART

Department of Chemistry, The Ohio State University, Columbus, Ohio 43210, USA

(Received 15 September 1983; accepted 20 December 1983)

Abstract. $M = \text{La, Ce, Pr, Nd, Sm, Eu, Gd, Tb, Dy, Ho, Er, Tm, Yb, Lu}$. Isomorphous, hexagonal $P6_3/m$, $Z = 2$, $\lambda(\text{Mo } K\alpha) = 0.71069 \text{ \AA}$. $M = \text{La}$: $M_r = 676.40$, $a = 14.045$ (1), $c = 7.0996$ (5) \AA , $V = 1212.8$ (2) \AA^3 , $D_x = 1.852 \text{ g cm}^{-3}$, $\mu = 20.97 \text{ cm}^{-1}$, $F(000) = 684$, $R = 0.020$, 1560 reflections. $M = \text{Lu}$: $M_r = 712.46$, $a = 13.834$ (1), $c = 6.9612$ (8) \AA , $V = 1153.8$ (3) \AA^3 , $D_x = 2.051 \text{ g cm}^{-3}$, $\mu = 46.30 \text{ cm}^{-1}$, $F(000) = 712$, $R = 0.020$, 1438 reflections. The lanthanide ions are coordinated by nine water molecules, with the coor-

dination polyhedron having $\bar{6}$ (C_{3h}) symmetry. The metal-oxygen distances decrease with increasing atomic number, and correlate well with the ionic radius of the metal. The ethyl sulfate ions are hydrogen-bonded to the water molecules coordinating the metal ion. Probability-plot analysis shows that the geometry of the ethyl sulfate ion is independent of both the structure and the temperature in the range 171–298 K. Hydrogen atoms were located using difference Fourier syntheses, and were successfully refined.

Introduction. The crystal structures of the lanthanide ethyl sulfate enneahydrates were first investigated by Ketelaar (1937), who assigned the space group $P6_3/m$ to the isomorphic series. Structure refinements for praseodymium and erbium (Fitzwater & Rundle, 1959), holmium (Hubbard, Quicksall & Jacobson, 1974), and praseodymium and ytterbium (Albertsson & Elding, 1977) ethyl sulfates have been subsequently reported, all confirming the original space-group assignment. In these studies, for only the Ho structure were all the hydrogen positions determined.

Recent interest in the crystal structures of these compounds has been due mainly to their use in EPR studies as hosts for dilutely substituted paramagnetic ions. A detailed knowledge of the host crystal structure and the use of the superposition model (Newman & Urban, 1972) allows the determination of host-independent spin-Hamiltonian parameters for a paramagnetic ion. Such an analysis was done for Gd^{III} in the lanthanide ethyl sulfates by Gerkin & Rogers (1979), using the limited structural data then available. This comprehensive examination of the lanthanide ethyl sulfate series (except promethium) was undertaken in part to provide accurate geometric details for each structure, so that an improved superposition model analysis could be performed for Gd^{III} in this crystal series.

Experimental. The ethyl sulfates of all the lanthanides except cerium were prepared by the hydrolysis (358 K) of an excess of diethyl sulfate in the presence of the metal oxide. Cerium(III) chloride was used for the preparation of cerium ethyl sulfate, since cerium oxide contains the tetravalent metal. Clear crystals having the shape of regular hexagonal prisms were cut from hexagonal columns obtained by slow evaporation at room temperature.

Crystals mounted on a Syntex $P\bar{1}$, automated, four-circle diffractometer with c nearly parallel to the diffractometer φ axis. Unit-cell parameters (171 K, graphite-monochromated $Mo K\alpha$ radiation) by a least-squares fit of the setting angles for 25 centered reflections ($19^\circ < 2\theta < 31^\circ$). Intensity data for the $+h$, $+k$, $+l$ reflections, $4^\circ \leq 2\theta \leq 60^\circ$, collected using the ω - 2θ scan technique. Uncertainties assigned to each reflection using $\sigma_f^2 = R^2(C + BT^2) + (0.02 I)^2$, where R is the scan rate, C is the total number of counts, T is the scan time/background time ratio, B is the total number of background counts, and I is the intensity. Six standard reflections measured periodically showed less than 0.4% crystal decay per hour of exposure. Lorentz-polarization and analytical absorption corrections applied for all salts except those of neodymium, samarium and erbium, for which empirical absorption corrections (ψ scans) were used. Reflections with $I \geq 3\sigma_f$, used in subsequent calculations. Unit-cell

Table 1. Unit-cell constants for the rare-earth ethyl sulfates at 171 K

	a (Å)	c (Å)	V (Å ³)
La	14.045 (1)	7.0996 (5)	1212.8 (2)
Ce	14.010 (1)	7.0860 (7)	1204.6 (3)
Pr	13.984 (2)	7.0754 (8)	1198.2 (3)
Nd	13.963 (1)	7.0644 (6)	1192.8 (2)
Sm	13.930 (1)	7.0468 (5)	1184.2 (2)
Eu	13.910 (1)	7.0350 (5)	1178.8 (2)
Gd	13.905 (1)	7.0249 (5)	1176.2 (2)
Tb	13.885 (1)	7.0187 (5)	1171.8 (2)
Dy	13.862 (1)	7.0122 (6)	1166.9 (2)
Ho	13.858 (1)	6.9972 (5)	1163.7 (2)
Er	13.850 (2)	6.9897 (8)	1161.1 (3)
Tm	13.845 (1)	6.9841 (6)	1159.3 (3)
Yb	13.834 (1)	6.9769 (6)	1156.2 (2)
Lu	13.834 (1)	6.9612 (8)	1153.8 (3)

dimensions and details of the data collection for each crystal are given in Tables 1 and 2.

The low temperature was maintained by a Syntex LT-1 low-temperature attachment, and was measured at the cold-stream exit nozzle during data collection and at the crystal site after data collection with a Fluke 2100A digital thermometer (Type K thermocouple). The temperature at the exit nozzle was maintained at 152 K, and fluctuated by only ± 0.3 K, except when the nitrogen tank was filling. During these times, the temperature would drop by as much as 5 K, but would return to 152 K over a period of 30 min. Since the nitrogen tank was refilled twice during data collection over a 24 h period, only about 4% of the data could in any way have been affected. The temperature measured at the site of the crystal was 171 K with an estimated overall uncertainty of ± 2 K.

The gadolinium ethyl sulfate data were subjected to the first analysis: Gd position determined from a Patterson map, all other non-hydrogen atoms located by subsequent difference syntheses. Full-matrix least-squares refinement (*SHELX76*, Sheldrick, 1976) minimizing $\sum w(|F_o| - |F_c|)^2$ ($w = 1/\sigma_f^2$) yielded $R = 0.030$ after inclusion of anisotropic thermal parameters. Additional refinement, including isotropic H atoms from a difference map, gave $R = 0.024$. An isotropic extinction coefficient, ϵ , $\{F_c' = F_c[1 - (\epsilon F_c^2 / \sin\theta)]\}$ was introduced into the calculation and refinement converged to the R and R_w values listed in Table 2.

Initial estimates for the parameters used in the refinement of the other structures were taken from the results for gadolinium ethyl sulfate. In each case, convergence was reached after four to five cycles of refinement. The final difference map for each structure was essentially featureless, with the largest peak (Table 2) being located near the site of the lanthanide ion.

Neutral-atom scattering factors for the lanthanides from Cromer & Waber (1965), those for C, O and S from Cromer & Mann (1968), H atom scattering factor from Stewart, Davidson & Simpson (1965). Corrections for anomalous dispersion included for S and the metal atoms (Cromer & Liberman, 1970).

Discussion. The final positional parameters and equivalent isotropic temperature factors are given in Tables 3 and 4, respectively.* Important interatomic distances and angles, calculated using the *XRAY* system (Stewart, Kruger, Ammon, Dickinson & Hall, 1972), are listed in Table 5.

The structure of each lanthanide ethyl sulfate consists of columns of hydrated metal ions centered on the $\bar{6}$ axes located at the positions $x = \pm \frac{1}{3}$, $y = \pm \frac{2}{3}$, and of columns of ethyl sulfate ions centered on the 6_3 axis located at the origin. The ethyl sulfate ions are linked by hydrogen bonds to the water molecules coordinating the metal ion.

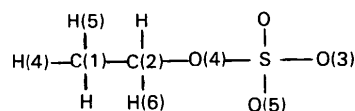
Each lanthanide ion is coordinated to nine water molecules. Six O(1) atoms are situated at the vertices of a trigonal prism, and three O(2) atoms lie in the mirror

* Lists of structure factors, anisotropic thermal parameters and bond lengths and angles have been deposited with the British Library Lending Division as Supplementary Publication No. SUP 39175 (78 pp.). Copies may be obtained through The Executive Secretary, International Union of Crystallography, 5 Abbey Square, Chester CH1 2HU, England.

Table 4. *Equivalent isotropic thermal parameters* ($\text{\AA}^2 \times 10^4$), calculated from the equation $U_{eq} = \frac{1}{3}(U_{11} + U_{22} + U_{33} - U_{12})$

	La	Ce	Pr	Nd	Sm	Eu	Gd	Tb	Dy	Ho	Er	Tm	Yb	Lu
<i>M</i>	90	86	88	78	79	81	81	80	87	79	76	80	80	85
<i>S</i>	121	116	116	106	106	107	109	106	112	82	96	105	104	106
O(1)	160	153	154	138	137	139	141	135	144	115	125	132	130	133
O(2)	155	142	140	128	131	129	137	138	140	105	126	131	134	136
O(3)	168	161	158	148	147	146	148	148	155	120	135	144	138	144
O(4)	187	187	178	168	166	171	170	172	170	135	161	157	170	171
O(5)	171	163	154	153	151	152	154	158	159	126	145	149	150	156
C(1)	280	280	277	253	252	252	251	251	253	214	229	240	245	254
C(2)	379	357	367	351	358	360	341	352	370	322	321	335	322	352

plane containing the metal ion. The O(2) atoms approximately cap the faces of the prism, and are at a greater distance from the metal ion than are the O(1) atoms. The symmetry of the coordinated ion is distorted from $\bar{6}m2$ (D_{3h}) to $\bar{6}$ (C_{3h}) as a result of the arrangement of the hydrogen bonds, which do not allow the O(2) atoms to be equidistant from the surrounding O(1) atoms. The angle required to rotate the O(2) atoms in the mirror plane to achieve $\bar{6}m2$ (D_{3h}) symmetry, φ_d , decreases with decreasing ionic radius* of the metal. The decreasing values of φ_d appear to result from the decreasing $M-O(1)$ and $M-O(2)$ distances, which would cause an increased repulsion between the closest O(1) and O(2) atoms, if no rotation occurred. A stereoview showing the environment of the gadolinium ion is given in Fig. 1. H(1) and H(2) are bonded to water oxygen O(1), H(3) to water oxygen O(2). The numbering of the ethyl sulfate ion is shown below:



The change in the geometry of the coordinated ion from lanthanum to lutetium correlates well with the ionic radius of the lanthanide ion. As shown in Fig. 2, the distances from the metal ion to O(1) and O(2) decrease regularly with the ionic radius. The smooth curves in the figure represent best-fit quadratic and linear dependences, respectively. The O(1)— M —O(1ⁱⁱ)

* The ionic radii were taken from Shannon (1976), and are valid for nine-coordinated lanthanide ions in halide and chalcogenide structures.

Table 5. *Selected interatomic distances* (\AA) *and angles* ($^\circ$)

Standard deviations are given within parentheses

	Coordination sphere						φ_d
	$M-O(1)$	$M-O(2)$	O(1)—O(2)	O(1)—O(2)	O(1)—O(1 ⁱⁱ)	O(1)— M —O(1 ⁱⁱ)	
La	2.517 (1)	2.616 (3)	2.770 (3)	3.058 (3)	3.531 (3)	89.09 (5)	5.93 (8)
Ce	2.491 (1)	2.600 (3)	2.753 (2)	3.034 (3)	3.509 (3)	89.55 (5)	5.86 (8)
Pr	2.470 (2)	2.583 (3)	2.735 (3)	3.009 (4)	3.483 (4)	89.69 (7)	5.76 (10)
Nd	2.457 (1)	2.570 (2)	2.726 (2)	2.995 (3)	3.475 (3)	90.01 (5)	5.71 (6)
Sm	2.430 (1)	2.550 (4)	2.704 (3)	2.966 (3)	3.444 (3)	90.28 (5)	5.62 (8)
Eu	2.415 (1)	2.542 (3)	2.695 (3)	2.952 (3)	3.428 (3)	90.42 (5)	5.54 (8)
Gd	2.401 (1)	2.536 (3)	2.683 (3)	2.940 (3)	3.402 (3)	90.22 (6)	5.56 (8)
Tb	2.382 (2)	2.527 (3)	2.673 (3)	2.920 (3)	3.379 (3)	90.35 (6)	5.40 (9)
Dy	2.371 (1)	2.517 (3)	2.661 (3)	2.909 (3)	3.369 (3)	90.57 (6)	5.45 (8)
Ho	2.362 (2)	2.511 (4)	2.654 (4)	2.901 (4)	3.357 (4)	90.59 (7)	5.44 (11)
Er	2.352 (2)	2.503 (3)	2.649 (3)	2.884 (4)	3.339 (4)	90.47 (7)	5.21 (10)
Tm	2.340 (2)	2.504 (5)	2.648 (3)	2.875 (5)	3.325 (5)	90.56 (8)	5.06 (14)
Yb	2.324 (2)	2.503 (3)	2.638 (3)	2.865 (3)	3.300 (3)	90.52 (6)	5.07 (9)
Lu	2.318 (2)	2.497 (3)	2.633 (3)	2.854 (4)	3.285 (4)	90.26 (7)	4.93 (10)
	Ethyl sulfate ion			Hydrogen bonds			
S—O(3)	1.454 (2)	O(3)—S—O(4)	102.09 (9)	O(1)—O(3)	2.739 (5)	O(1)—H(1)—O(3)	172 (3)
S—O(4)	1.578 (2)	O(3)—S—O(5)	113.33 (8)	O(1)—O(5 ⁱⁱ)	2.805 (2)	O(1)—H(2)—O(5 ⁱⁱ)	166 (3)
S—O(5)	1.453 (2)	O(4)—S—O(5)	107.31 (8)	O(2)—O(5 ⁱⁱ)	2.848 (2)	O(2)—H(3)—O(5 ⁱⁱ)	168 (5)
O(4)—C(2)	1.460 (3)	O(5)—S—O(5 ⁱⁱ)	112.6 (2)				
C(1)—C(2)	1.475 (5)	S—O(4)—C(2)	116.2 (3)				
C(1)—H(4)	0.95 (4)	O(4)—C(2)—C(1)	109.1 (2)				
C(1)—H(5)	0.82 (7)	H(4)—C(1)—H(5)	106 (4)				
C(2)—H(6)	0.98 (4)	H(5)—C(1)—H(5 ⁱⁱ)	104 (8)				
		H(6)—C(2)—H(6 ⁱⁱ)	82 (10)				
				Water molecules			
				O(1)—H(1)	0.86 (5)	H(1)—O(1)—H(2)	103 (4)
				O(1)—H(2)	0.75 (5)	H(3)—O(2)—H(3 ⁱⁱ)	98 (5)
				O(2)—H(3)	0.81 (4)		

Code for symmetry-related atoms: (i) $y - x$, $1 - x$, z ; (ii) x , y , $\frac{1}{2} - z$; (iii) x , y , $\frac{3}{2} - z$; (iv) y , $1 + y - x$, $z - \frac{1}{2}$.

angle increases from La to Lu as a result of the decreasing $M-O(2)$ distance, which forces the O(1) atoms up. It is interesting to note, however, that in a plot of this angle *versus* the ionic radius of the trivalent metal, breaks occur in the curve at the gadolinium and lutetium ions, which have half-full and full 4*f* shells, respectively.

Comparison of the geometry of the coordinated ion at 171 K with the geometry at room temperature (Albertsson & Elding, 1977) shows that the only significant difference is a decrease in φ_d with an increase in temperature: 5.76 to 5.03° for praseodymium ethyl sulfate, and 5.07 to 4.77° for ytterbium ethyl sulfate.

The mirror planes at $z = \pm \frac{1}{4}$ contain the O(3)–S–O(4)–C(2)–C(1)–H(4) chain of the ethyl sulfate ions, with the O(5), H(5) and H(6) atoms lying above and below these planes. Hydrogen bonds from O(3) to H(1) and from O(5) to both H(2) and H(3) link the ethyl sulfate ions to the coordinated metal ions, with

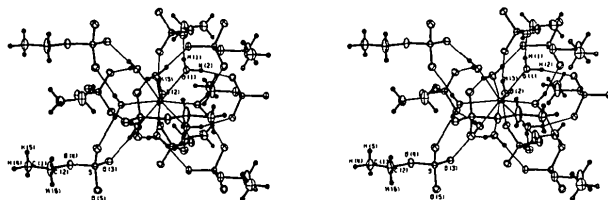


Fig. 1. Stereoview of the environment of the metal ion in gadolinium ethyl sulfate. Thermal ellipsoids are drawn at 50% probability for all atoms except hydrogen, for which the ellipsoid size has been set artificially small.

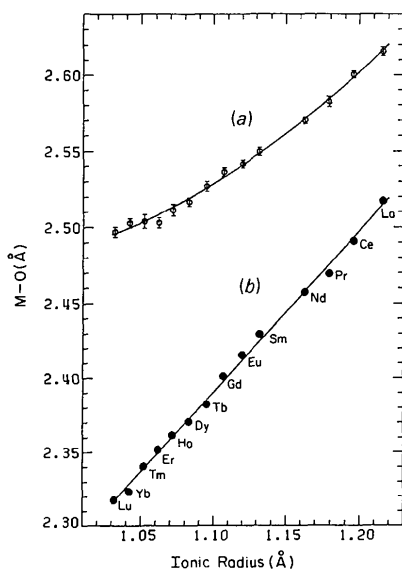


Fig. 2. Metal–oxygen distance *vs* the ionic radius of the metal: (a) $M-O(2)$; (b) $M-O(1)$. The smooth curves represent best-fit quadratic and linear dependences, respectively. The magnitudes of the error bars in (b) are less than the symbol diameter.

each O(3) and O(5) participating in two hydrogen bonds.

Comparison of bond lengths and angles suggested that the ethyl sulfate ion might have the same geometry in each structure, as was shown in the structures studied at room temperature by Albertsson & Elding (1977). To test this hypothesis, a half-normal probability-plot analysis (Abrahams & Keve, 1971; De Camp, 1973) was performed on all possible (91) pairs of ethyl sulfate ions, using interatomic distances

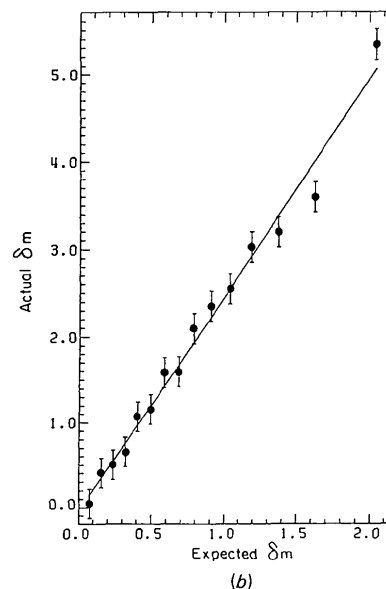
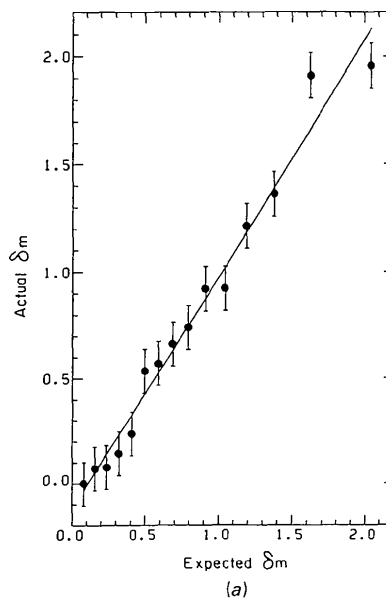


Fig. 3. Typical half-normal probability plots for the ethyl sulfate ion in (a) Nd and Eu ethyl sulfate at 171 K and (b) Pr ethyl sulfate at 171 and 296 K (Albertsson & Elding, 1977). The error bars represent the standard deviation of the fit.

between non-hydrogen atoms up to 4.5 Å. The resulting plots were linear, with slopes near one and y intercepts near zero (Fig. 3a). These results indicate that the differences in the interatomic distances are normally distributed, and that there are no systematic differences in the ethyl sulfate ion geometry in any of the lanthanide ethyl sulfate structures studied. For this reason, the interatomic distances and angles for the ethyl sulfate ion listed in Table 5 are average values, determined from the results of all 14 structures. The standard deviations listed are those about the mean values. An analysis using distances for the ethyl sulfate ion at 171 K and at room temperature gave similar results (Fig. 3b), except that the slopes were near two, indicating a discrepancy in the standard deviations.

The distance and angle values given in Table 5 for the water molecules and the hydrogen bonds are average values determined from all 14 structures. Average values are reported here because (1) the H-atom parameters were the least well-determined parameters in the structures and (2) all individual values agreed with the corresponding mean values, according to the following distribution: 73% agreed with the mean value to within 1 standard deviation, 93% agreed within 2 standard deviations, and 98% agreed to within 3 standard deviations. A complete list of bond distances for all structures has been deposited along with the structure factors.

Although for the purposes of the present paper we have employed ionic radii of the lanthanides as given by Shannon (1976), the present data afford the possibility of an independent assignment of radii based on data from a single study of a series of salts of all the lanthanides (except Pm). An analysis of this matter is planned for a later paper.

The authors would like to thank Wilson H. De Camp for providing us with a copy of his probability-plot analysis program, on which ours was largely based, and Alan P. Lundstedt for the use of his plotting program *APL PLOT II* (Lundstedt, 1983). We would especially like to thank Dr Judith C. Gallucci, who gave us invaluable advice at every stage of this project. Computational facilities were provided by the Ohio State University IRCC.

References

- ABRAHAMS, S. C. & KEVE, E. T. (1971). *Acta Cryst.* **A27**, 157–165.
 ALBERTSSON, J. & ELDING, I. (1977). *Acta Cryst.* **B33**, 1460–1469.
 CROMER, D. T. & LIBERMAN, D. (1970). *J. Chem. Phys.* **53**, 1891–1898.
 CROMER, D. T. & MANN, J. B. (1968). *Acta Cryst.* **A24**, 321–324.
 CROMER, D. T. & WABER, J. T. (1965). *Acta Cryst.* **18**, 104–109.
 DE CAMP, W. H. (1973). *Acta Cryst.* **A29**, 148–150.
 FITZWATER, D. R. & RUNDLE, R. E. (1959). *Z. Kristallogr.* **112**, 362–374.
 GERKIN, R. E. & ROGERS, W. J. (1979). *J. Chem. Phys.* **70**, 3764–3774.
 HUBBARD, C. R., QUICKSALL, C. O. & JACOBSON, R. A. (1974). *Acta Cryst.* **B30**, 2613–2619.
 KETELAAR, J. A. A. (1937). *Physica (Utrecht)*, **8**, 619–630.
 LUNDSTEDT, A. P. (1983). *APL PLOT II, a Digital Computer Plotting System*. The Ohio State Univ., Columbus, Ohio.
 NEWMAN, D. J. & URBAN, W. (1972). *J. Phys. C*, **5**, 3101–3109.
 SHANNON, R. D. (1976). *Acta Cryst.* **A32**, 751–767.
 SHELDRIK, G. M. (1976). *SHELX76*. A program for crystal structure determination, Univ. Chemical Laboratory, Cambridge, England.
 STEWART, J. M., KRUGER, G. J., AMMON, H. L., DICKINSON, C. W. & HALL, S. R. (1972). The *XRAY* system – version of June 1972. Tech. Rep. TR-192. Computer Science Center, Univ. of Maryland, College Park, Maryland.
 STEWART, R. F., DAVIDSON, E. R. & SIMPSON, W. T. (1965). *J. Chem. Phys.* **42**, 3175–3187.

Acta Cryst. (1984). **C40**, 786–788

Structure of Tricarbonylbis(triphenylphosphine)ruthenium(0)–Tetrahydrofuran (2/1), $[\text{Ru}(\text{CO})_3\{\text{P}(\text{C}_6\text{H}_5)_3\}_2] \cdot 0.5\text{C}_4\text{H}_8\text{O}$

BY FRANÇOISE DAHAN, SYLVIANE SABO AND BRUNO CHAUDRET

Laboratoire de Chimie de Coordination du CNRS, associé à l'Université Paul Sabatier, 205 route de Narbonne,
 31400 Toulouse, France

(Received 14 October 1983; accepted 27 January 1984)

Abstract. $M_r = 745$, monoclinic, $P2_1/c$, $a = 17.845$ (2), $b = 12.315$ (2), $c = 18.351$ (3) Å, $\beta = 104.55$ (1)°, $V = 3903.5$ (4) Å³, $Z = 4$, $D_x = 1.27$ Mg m⁻³, $\lambda(\text{Mo } K\alpha) = 0.71069$ Å, $\mu = 0.51$ mm⁻¹, $F(000) = 1528$, $T = 293$ K. Final $R = 0.045$ for 2894 observed reflections. Ru is fivefold coordinated, the three carbonyls being in

the equatorial plane and the P atoms of the triphenylphosphines at the apices of a rather regular trigonal bipyramid, the preferred configuration for complexes in low oxidation states. The structure can be considered as $[\text{Ru}(\text{CO})_3(\text{PPh}_3)_2]$ units with tetrahydrofuran molecules stabilizing the crystal packing.